JOURNAL OF SOLID STATE CHEMISTRY 27, 105–114 (1979)

Fluorite-Related Phases Ln_3MO_7, Ln = Rare Earth, Y, or Sc, M = Nb, Sb, or Ta. I. Crystal Chemistry

J. G. ALLPRESS AND H. J. ROSSELL*

CSIRO, Division of Materials Science, Engineering Ceramics and Refractories Laboratory, P.O. Box 4331, GPO, Melbourne 3001, Victoria, Australia

Received March 11, 1978

Compounds Ln_3MO_7, where Ln = La, Nd, Gd, Ho, Er, Y, or Sc, and M = Nb, Ta, or Sb have been examined by powder X-ray diffraction, electron diffraction, and electron microscopy. For large Ln cations, an orthorhombic fluorite-related superstructure is formed, of probable space group $Cmcm$ for Ln = La and $C222_1$ for Ln = Nd, Gd, Ho, or Y, while for the smaller Ln cations, Er, and under some conditions, Ho and Y, the structure is defect fluorite containing microdomains of ordered, but undetermined, structure. The composition Sc_3MO_7 was not single phase under the conditions used. Compounds of the type Ln_2ScMO_7 have the pyrochlore structure.

Introduction

Compounds of composition Ln_3MO_7, where Ln is a group IIIa or rare earth ion, and M is Nb, Ta, or Sb, have been studied by several groups of workers. Two crystallographically distinct structure types have been reported.

(a) A defect fluorite-type structure was found by Rooksby and White (*1*) for a number of Ln_3NbO_7 and Ln_3TaO_7 materials for which the Ln cation was smaller than Nd^{3+}. They suggested the possibility of pyrochlore ordering, but found no positive evidence for this in their X-ray diffraction data. Nath (*2*), working with Ln_3SbO_7, asserted that for Ln = Nd, Sm, Eu, Gd, Tb, Dy, Ho, Er, Tm, Yb, or Y, the structure was that of pyrochlore, but presented no evidence for this: The published X-ray powder pattern of Gd_3SbO_7, stated to be representative of all these compounds, contained no extra reflections typical of pyrochlore ordering, but only those of fluorite with arbitrarily doubled indices. Antimonates of the type $Ln_2Ln'SbO_7$, Ln = Y, Gd, Lu; Ln' = Y, Gd, Lu, Ga also have been described as pyrochlores (*3*, *4*).

(b) An orthorhombic structure has been reported for Ln_3MO_7 compositions with larger Ln cations. Rooksby and White (*1*) concluded that the structure was related to that of weberite (*5*), space group $Imm2$, on the basis of a comparison of the X-ray powder data with that of $Ca_2Sb_2O_7$ (*6*). Tilloca *et al.* (*7*) reported orthorhombic unit cells of similar dimensions to the above for Ln_3NbO_7 with Ln = La, Nd, or Sm, stating the space group to be $Pnam$, and noting that these orthorhombic phases transform to structures of higher symmetry at high temperatures.

This series of compounds was considered worthy of further study in order to search for ordering in the cubic phases using the sensitive technique of electron diffraction, and to determine the correct space group and structure of the orthorhombic phases. The work will be reported in three parts:

I. Preparation and crystal chemistry of the

* Author to whom enquiries should be addressed.

0022-4596/79/0271/0105/10/$02.00/0

phases Ln_3MO_7, including powder X-ray diffraction and electron-optical studies,

II. Structure determination of four compounds representative of the orthorhombic Ln_3MO_7 phase,

III. An investigation of apparent non-stoichiometry in orthorhombic Y_3TaO_7.

Experimental

The oxides used as starting materials were all at least 99.9% pure, with the exception of Ta_2O_5 which was described as optical grade, Sb_2O_3 (laboratory reagent), and Sc_2O_3 which was nominally 99.5% pure. Sources of supply were Atomergic Chemetals (oxides of Nd, Gd, Ho, Er and Y), Koch-Light Ltd. (Nb_2O_5), Kawecki Berylco Ind. Inc. (Ta_2O_5), Thorium Ltd. (La_2O_3), Australian Mineral Development Lab. (Sc_2O_3) and British Drug Houses Ltd. (Sb_2O_3). The rare earth and scandium oxides were purified further by two precipitations from nitric acid solution as oxalate, followed by ignition to the oxide.

All oxides were calcined at 1000°C before use. Weighed quantities of oxides were milled together under acetone in an agate mortar, and pressed into small pellets.

Tantalate and niobate preparations were sintered in air at 1400°C for 2 weeks, or at 1600°C for 40 hr, or were arcmelted in an argon atmosphere. Appropriate annealing was carried out subsequently. Shorter sintering times resulted in incomplete reaction, and the specimens contained, in addition to the required products, small amounts of the mono-

TABLE I

UNIT CELL DIMENSIONS OF ORTHORHOMBIC Ln_3MO_7

Compound	a (Å)	b (Å)	c (Å)	Space group	Reference
La_3TaO_7	11.173(2)[a]	7.619(1)	7.755(1)	*Cmcm*	this work
	7.84	10.86	7.70	*Imm*2	(*1*)
La_3NbO_7	11.167(1)	7.629(1)	7.753(1)	*Cmcm*[b]	this work
	7.84	10.86	7.76	*Imm*2	(*1*)
	7.62	7.76	11.15	*Pnam*	(*7*)
La_3SbO_7	11.1509(7)	7.6299(5)	7.7424(5)	*Cmcm*	this work
Nd_3TaO_7	10.818(2)	7.614(1)	7.683(1)	$C222_1$	this work
	7.66	10.98	7.52	*Imm*2	(*1*)
Nd_3NbO_7	10.905(2)	7.517(2)	7.624(1)	*Cmcm*[c]	this work
	7.66	10.98	7.52	*Imm*2	(*1*)
	7.52	7.63	10.91	*Pnam*	(*7*)
Gd_3TaO_7	10.623(2)	7.527(2)	7.548(1)	$C222_1$	this work
Gd_3NbO_7	10.610(1)	7.521(1)	7.550(1)	$C222_1$	this work
Ho_3TaO_7	10.487(2)	7.430(1)	7.450(2)	$C222_1$	this work
Y_3TaO_7	10.4762(7)	7.4237(7)	7.4522(5)	$C222_1$[b]	this work
Y_3SbO_7	10.484(1)	7.493(1)	7.424(1)	$C222_1$	this work
Y_2GdTaO_7	10.523(1)	7.456(1)	7.485(1)	$C222_1$	this work
Y_2GdSbO_7	10.5172(6)	7.4527(5)	7.4806(4)	$C222_1$[b]	this work
YGd_2NbO_7	10.559(1)	7.482(1)	7.518(1)	$C222_1$	this work
$Ca_2Sb_2O_7$	7.2974(5)	7.4625(5)	10.2091(6)	*I****	this work
	7.28	7.44	10.18	*Imm*2	(*5*)

[a] Numbers in parentheses are standard deviations calculated from measurements of individual patterns, and refer to the last quoted place.

[b] Space group confirmed by structure determination. Those space groups not marked are inferred: Their diffraction symbols at least are correct.

[c] Symmetry according to X-ray structure determination. The true symmetry is $C222_1$ type.

clinic $LnMO_4$ fergusonite phase (*8*) and of M_2O_3, as shown by X-ray powder patterns. Apart from this effect, X-ray powder patterns from a given material either sintered or arc-melted and annealed, were indistinguishable.

Preparations of antimonates were made with about 10% excess Sb_2O_3 to allow for volatilization: They were heated in air at 960°C for 16 hr, and then reground, repelleted, and heated in air at 1200°C for 24 hr, then 1350°C for 72 hr (*3*). Oxidation of antimony to Sb^v occurred during this process.

A specimen of Nd_3NbO_7 was made by the coprecipitation method of Vladimirova *et al.* (*9*) and fired at 1400°C for 2 weeks. The product differed from Nd_3NbO_7 prepared by the other methods only in the crystallite size, which was too small for convenient manipulation in the electron microscope.

The compound $Ca_2Sb_2O_7$ of the weberite (Na_2MgAlF_7) structure was prepared by the reaction of analytical reagent $CaCO_3$ and Sb_2O_3 at 1200°C for 24 hr.

Electron diffraction patterns from single crystal fragments of the products, prepared by crushing and dispersing on carbon-coated grids, were recorded using a JEM 200A electron microscope fitted with a tilting stage and operated at 200 kV. These data were used to establish the symmetry of the unit cells.

X-ray powder diffraction patterns were recorded in a Guinier focusing camera, using Cu$K\alpha_1$ radiation, and thoria, $a = 5.5972$ Å, as an internal standard. Unit cell dimensions were obtained from these patterns using a least-squares procedure.

Results and Discussion

Most of the Ln_3MO_7 specimens examined in this study were single phases, and of either orthorhombic or cubic structure. The excep-

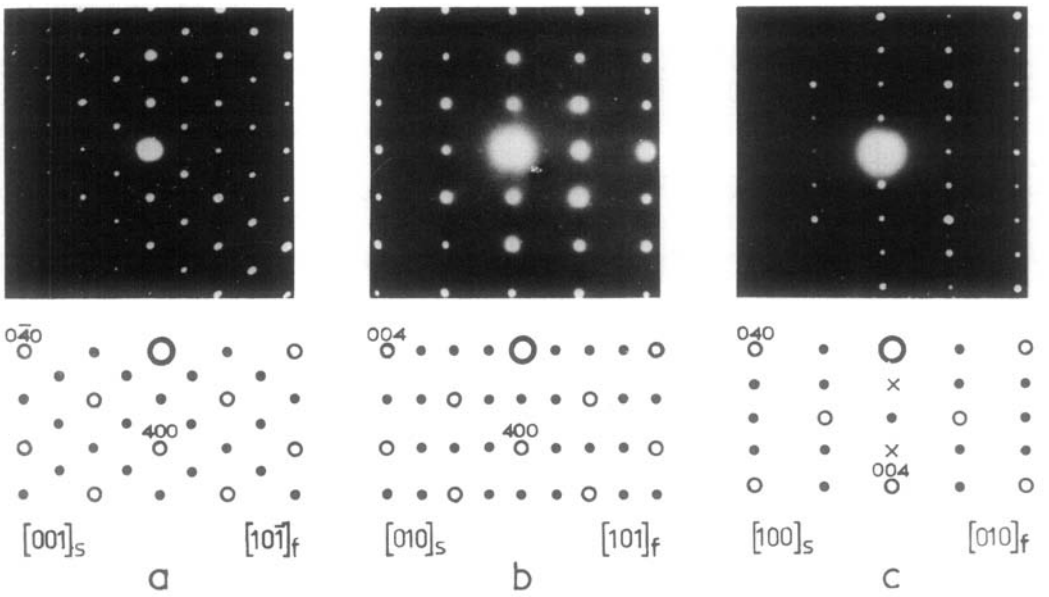

FIG. 1. Electron diffraction patterns typical of the orthorhombic phase Ln_3MO_7. The material is Nd_3TaO_7 prepared by sintering the component oxides at 1400°C for 21 days. In the diagrams, open circles represent subcell spots, filled circles, the supercell spots; and crosses, spots that should be systematically absent in patterns from La_3MO_7, but which appear because of double diffraction. The subscripts *s* and *f* refer to supercell and subcell, respectively. In (b), supercell reflections *h*0*l* for *l* odd are very weak: They are absent in La_3MO_7, but much stronger in Ln_3MO_7, Ln ≠ La, Nd.

tions were materials containing scandium, and these will be discussed separately below.

1. The Orthorhombic Phase

1.1. Crystallography

Table I summarizes the crystallographic data for the orthorhombic phases examined here, with comparisons with the results of the previous workers.

The materials are superstructure phases based on a (distorted) face-centered cubic, fluorite-type subcell: This subcell gives rise to prominent reflections in both the X-ray and electron diffraction patterns. The axial relationship between supercell and subcell, viz.,

$$\begin{pmatrix} a \\ b \\ c \end{pmatrix} = \begin{pmatrix} 2 & 0 & 0 \\ 0 & 1 & 1 \\ 0 & -1 & 1 \end{pmatrix} \begin{pmatrix} a_1 \\ a_2 \\ a_3 \end{pmatrix}, \ldots \qquad (1)$$

was determined from electron diffraction patterns of a single crystal that had been tilted to at least two known subcell orientations on a zone, and was confirmed for all materials.

Figure 1 contains some examples of the single-crystal electron diffraction patterns obtained from the orthorhombic phases. For all the compounds, reflections hkl were systematically absent for $h + k \neq 2n$. For La_3MO_7 only, reflections $h0l$ for l odd were absent also, although for Nd_3NbO_7 and Nd_3TaO_7 they were extremely weak (Fig. 1b). Thus the space group for orthorhombic La_3MO_7 may be *Cmcm* (No. 63, D_{2h}^{17}), $Cmc2_1$ (No. 36, C_{2v}^{12}) or *C*2*cm* (an alternative setting of *Ama*2, No. 40, C_{2v}^{16}), while for the remaining compounds, the possible space groups are *Cmmm* (No. 65, D_{2h}^{19}), *Cm*2*m*, or *C*2*mm* (settings of *Amm*2, No. 38, C_{2v}^{14}), *Cmm*2 (No. 35, C_{2v}^{11}) or *C*222 (No. 21, D_2^6). The space group $C222_1$ (No. 20, D_2^5) must be added to this latter list, since the condition l even for reflections $00l$ may be obscured by double diffraction in the electron diffraction patterns. This condition existed in the X-ray powder patterns, although it cannot be regarded as established by this technique.

Structure refinement of La_3NbO_7, Nd_3NbO_7, Y_3TaO_7, and Y_2GdSbO_7, based on powder X-ray intensities (described in detail in Part II) were successful only with the space groups *Cmcm* for La_3NbO_7 and $C222_1$ for Y_3TaO_7 and Y_2GdSbO_7. In the case of Nd_3NbO_7, satisfactory refinement could not be achieved in any of the indicated space groups, nor in $C222_1$, but refinement in *Cmcm* was successful, a result which is not unexpected considering that in this case, the reflections $h0l$ for l odd are very weak. The space groups of the remaining compounds were inferred from the above on the basis that equivalent diffraction symbols implied similar space groups.

The present assignment of symmetry is at variance with the previous reports, but it is more likely to be correct, since it is consistent with the single-crystal electron diffraction data, and with detailed measurements of X-ray powder patterns.

The Guinier X-ray photographs of the various specimens showed marked differences in the intensities of supercell lines and in the separation of split subcell lines. The presence of few visible supercell lines and of poorly resolved groups of subcell lines in an X-ray powder pattern was one cause of the relatively large calculated standard deviations of the lattice parameters for several of the compounds.

It could be seen that given patterns of relatively poor resolution, groups of substructure lines and some superstructure lines could be taken as due to the pyrochlore structure. Also, the *C*-centered orthorhombic structure discussed above, and the body-centred orthorhombic weberite structure have the same subcell/supercell relationship, so that their powder patterns have the subcell lines and many supercell lines in common, and thus appear remarkably alike. These effects perhaps contributed to the earlier assignments of structure type mentioned above.

TABLE II

LATTICE PARAMETERS OF THE ORTHORHOMBIC PHASE IN SPECIMENS OF DIFFERENT OVERALL COMPOSITION

Composition	a (Å)	b (Å)	c (Å)	V (Å)^3
Y_3TaO_7	10.4762(7)	7.4237(7)	7.4522(5)	579.6(1)
$7Y_2O_3 \cdot 3Ta_2O_5$	10.4670(8)	7.3798(5)	7.4337(5)	573.4(1)
Ho_3TaO_7	10.487(2)	7.430(1)	7.450(2)	580.5(3)
$7Ho_2O_3 \cdot 3Ta_2O_5$	10.471(2)	7.385(1)	7.427(1)	574.3(3)
Gd_3TaO_7	10.625(1)	7.5236(9)	7.5510(6)	603.6(2)
$7Gd_2O_3 \cdot 3Ta_2O_5$	10.620(1)	7.4891(6)	7.5344(5)	599.2(2)
Gd_3NbO_7	10.610(1)	7.521(1)	7.550(1)	602.5(2)
$7Gd_2O_3 \cdot 3Nb_2O_5$	10.606(1)	7.514(1)	7.548(1)	601.6(2)
Nd_3NbO_7	10.905(2)	7.517(2)	7.624(1)	625.0(4)
$7Nd_2O_3 \cdot 3Nb_2O_5$	10.902(1)	7.518(1)	7.624(1)	624.9(2)

1.2. Nonstoichiometry

Table II contains the lattice parameters of some orthorhombic materials from specimens of overall composition 70 and 75 mole% Ln_2O_3. The orthorhombic Ln_3MO_7 phase coexists with a fluorite-type phase or Ln_2O_3 at overall compositions above 75 mole% Ln_2O_3, while at a sufficiently low Ln_2O_3 content, it coexists with the monoclinic $LnMO_4$ fergusonite phase. The 70 mole% Ln_2O_3 materials all contained $LnMO_4$ in various amounts, the smallest being for Ta_2O_5—70 mole% Y_2O_3 and the largest for Nb_2O_5—70 mole% Nd_2O_3. The lattice parameter variations indicate a relatively large homogeneity range for the Y_3TaO_7 and Ho_3TaO_7 phases, but much narrower ranges for Nd_3NbO_7 and the other materials investigated. The situation for the Y_3TaO_7 and Ho_3TaO_7 phases is not simple, however, as at the low-Ln_2O_3 side of their composition ranges, they have an entirely new orthorhombic structure. A detailed examination of the nonstoichiometric Y_3TaO_7 phase has been made, and it will be reported in Part III.

1.3. Order–Disorder Transformation

Specimens of Ho_3TaO_7 were of orthorhombic structure if prepared at or below 1400°C, but of cubic fluorite-type structure if prepared at 1600°C. On annealing at 1400°C, this cubic structure slowly transformed to the orthorhombic structure, the process being complete in about a week. The compound Y_3TaO_7 similarly exhibited a reversible cubic–orthorhombic transformation at 1600°C, but there were additional observations of complex nature. This material will be discussed further below.

Electron diffraction patterns from samples of Ln_3TaO_7 and Ln_3NbO_7, Ln = La, Nd, and Gd, that had been arc-melted and quenched, showed evidence for crystallites of orthorhombic superstructure existing in several orientations, but with a common subcell orientation. Some examples are shown in Fig. 2, together with a dark-field image to illustrate the typical domain structure of such specimens.

This result suggests that the orthorhombic superstructure is produced by way of a transformation during cooling. The fact that Ho_3TaO_7 and Y_3TaO_7 are cubic above 1600°C but orthorhombic at 1400°C indicates that the cubic structure is probably the high temperature form in these other cases also. It is further probable that the transformation temperature decreases as the radius of the Ln cation decreases, and is sufficiently low for the smallest Ln cation (Er) to render the transformation too slow to be observed (see below).

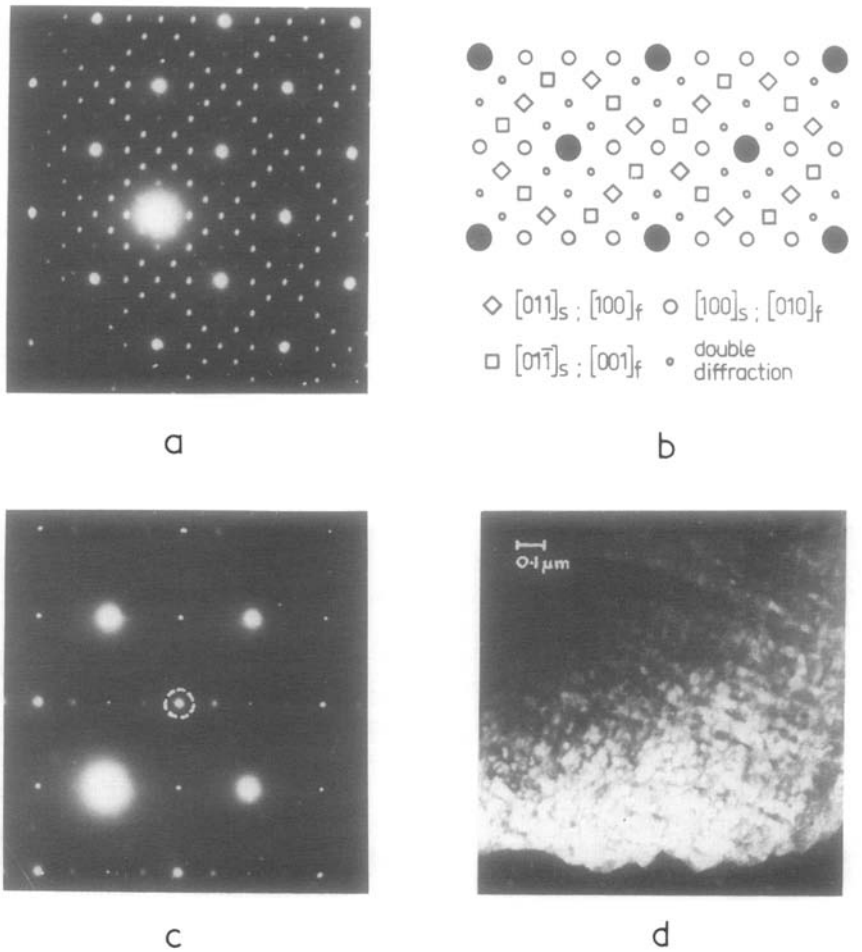

FIG. 2. (a) Electron diffraction pattern from arc-melted and quenched Nd_3TaO_7. (b) An analysis of (a) in terms of three orientations of the supercell coexisting within the same subcell orientation. (c) Electron diffraction pattern from arc-melted and quenched Gd_3TaO_7. The beam direction is $[332]_f$. (d) Dark-field image of the crystal in (c) formed with the circled supercell reflection, illustrating the domain structure typical of melted and quenched La_3MO_7, Nd_3MO_7, and Gd_3MO_7.

2. The Cubic Phase

A defect fluorite-type structure was observed for materials of composition Ln_3MO_7 when the radius of the Ln cation was small (Ln = Er, Y, Ho): All attempts to induce ordering in Ho_3NbO_7, Y_3NbO_7, Er_3TaO_7, and Er_3NbO_7 by annealing at 1400, 1200, and 1000°C for up to 1200 hr were unsuccessful. Lattice parameters are given in Table III. This phase is nonstoichiometric, and will tolerate a deficiency in Ln_2O_3, which results in a reduction in cell parameter. However, the extent of

TABLE III

UNIT CELL DIMENSIONS OF CUBIC Ln_3MO_7

Fluorite		Pyrochlore	
Composition	a (Å)	Composition	a (Å)
Ho_3TaO_7[a]	5.2581(2)	$YGdScSbO_7$	10.3836(4)
Ho_3NbO_7	5.2575(4)	La_2ScNbO_7	10.6723(4)
$ErTaO_7$	5.2390(2)	Nd_2ScNbO_7	10.5336(3)
Er_3NbO_7	5.2386(1)		
Y_3TaO_7[a]	5.2583(2)		
Y_3NbO_7	5.2561(4)		

[a] Quenched from 1600°C.

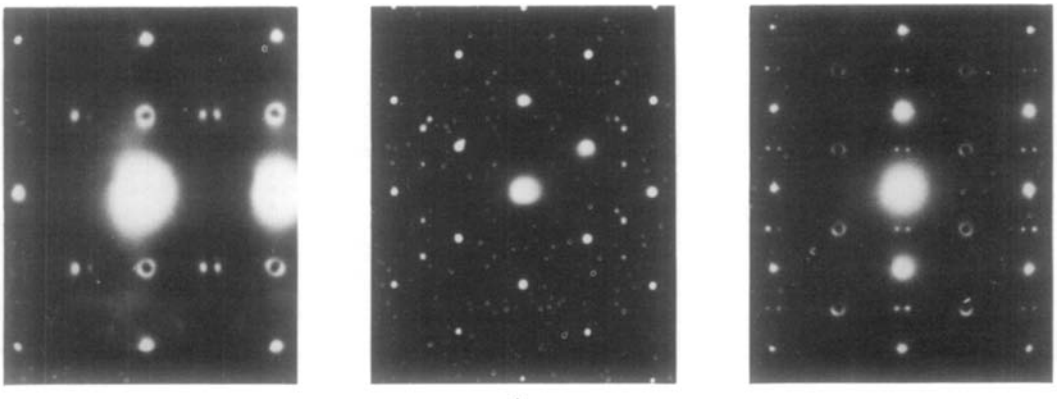

FIG. 3. Electron diffraction patterns typical of the cubic Ln_3MO_7 phases. The material is Er_3TaO_7 sintered at 1600°C for 40 hr and annealed at 1200°C for 145 hr. Corresponding patterns from the other cubic Ln_3MO_7 phases are indistinguishable from these. The beam directions are (a) [332], (b) [110], (c) [211].

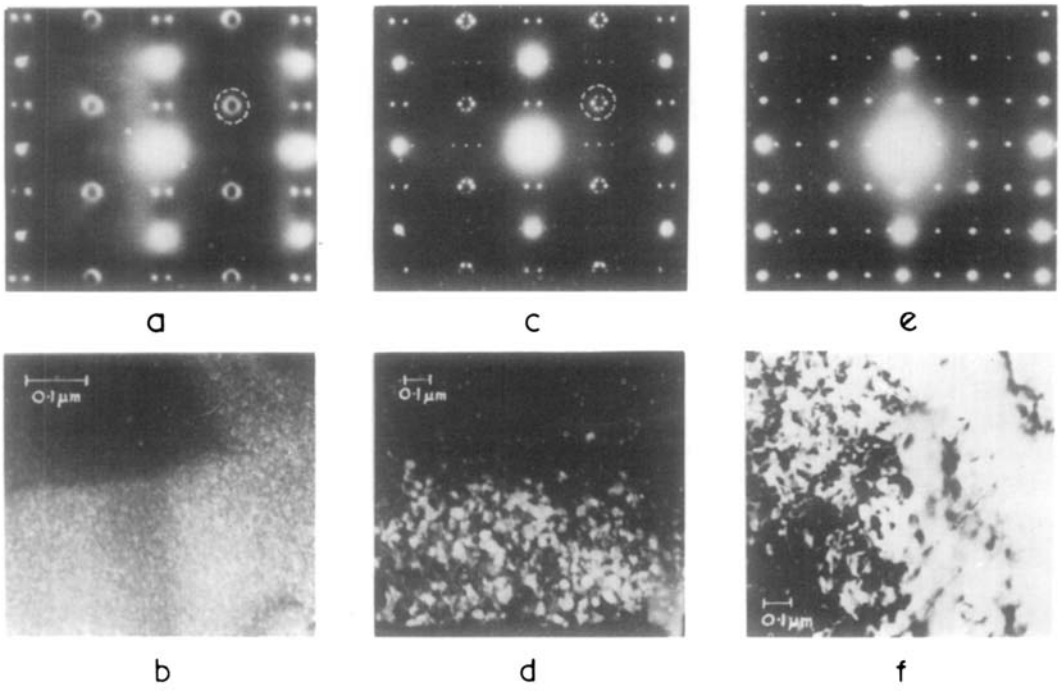

FIG. 4. Electron optical observations on Y_3TaO_7. (a) [211] (cubic) diffraction pattern from an arc-melted sample annealed at 1300°C for 215 hr. (b) Dark-field image from the same sample, formed with the circular feature outlined in (a), revealing the presence of domains of about 30-Å diameter. (c) [211] (cubic) pattern from an arc-melted specimen after annealing at 1400°C for 170 hr. (d) Dark-field image from the same sample, formed with the group of reflections outlined in (c). The domain size is about 400 Å. (e) [211] (subcell) pattern from part of a crystal from the same preparation as (c), showing superlattice spots characteristic of the orthorhombic phase. Apart from the subcell spots, there is no correspondence with the pattern in (c). (f) Bright-field image from the same crystal. The mottled contrast on the left is due to domains of the orthorhombic phase: The corresponding diffraction pattern is shown in (e). The diffraction pattern from the area on the right was similar to that in (c).

the homogeneity range was not determined for any of these materials.

Figure 3 shows some electron diffraction patterns typical of this fluorite phase. In addition to the strong reflections from the fluorite structure, there are numerous weaker and more diffuse features. The positions of these features do not bear any relationship to those of the superstructure spots of the orthorhombic phase, nor to those of the extra reflections which would be expected from the pyrochlore structure.

Figures 4a and b show an electron diffraction pattern and corresponding dark-field micrograph imaged with one of the diffuse circles, from a specimen of Y_3TaO_7 that had been arc-melted and annealed at 1300°C for 215 hr. The mottled appearance of the image contrast is evidence that the diffuse diffraction features arise from a microdomain structure, the domain size being of the order of 30 Å. The situation is analogous to our earlier results on $CaO–ZrO_2$ (*10*), and may have a similar interpretation, *viz.*, superstructure microdomains existing in a set of fixed orientations coherent with a fluorite-type matrix. The geometry of the diffuse patterns in the present case is different from that observed for $CaO–ZrO_2$, so that the superstructure of the microdomains must be different also.

Annealing of cubic Y_3TaO_7 (which gave patterns such as in Fig. 4a) for up to 170 hr at 1400°C resulted in the replacement of the diffuse features in the electron diffraction patterns by sharp spots in similar positions (Fig. 4c), and a corresponding increase in domain size to about 400 Å was indicated in dark-field images formed from a circle of these spots (Fig. 4d). Longer periods of annealing at 1400°C did not result in growth of these domains to a size such that single-crystal patterns could be studied in order to identify this superstructure, but instead, there was a conversion to the orthorhombic phase (Fig. 4e). The conversion would seem to have been relatively sudden, since grains could be found in which the 400-Å domain structure coexisted with regions of the orthorhombic phase. Figure 4f shows a bright-field image from such a crystal in the [211] subcell orientation, in which the mottled region on the left contains orthorhombic domains in several orientations, and the region on the right is similar to that shown in dark field in Fig. 4d. Electron diffraction patterns from the two regions are similar to those of Figs. 4e and c, respectively.

Other orientations of the structure which gave patterns of the kind shown in Fig. 4c indicated the presence of a long-period superlattice. As yet, no satisfactory interpretation of these data has been made. The above recrystallization phenomena were not observed in any of the other Ln_3MO_7 materials.

3. Ln_3MO_7 Containing Scandium

For specimens of composition Sc_3NbO_7 and Sc_3TaO_7, the products of reaction were monoclinic $ScMO_4$ and a rhombohedral fluorite-related superstructure phase isomorphous with $Zr_3Sc_4O_{12}$ (*11*) of composition $Sc_{5.5}M_{1.5}O_{12}$. The crystal structure of the niobium compound has been described (*12*).

The existence of cubic Sc_3MO_7, reported by Rooksby and White (*1*), therefore is not confirmed. The above result is more in accord with the observations of Vladimirova *et al.* (*9*), who found that specimens of overall composition Sc_3MO_7 consisted of $ScMO_4$ and a second rhombohedral phase whose composition could not be determined precisely, but which was estimated to be $Sc_6MO_{11.5}$. The lattice parameters (hexagonal) of $Sc_6NbO_{11.5}$ are $a = 9.278$, $c = 8.730$ Å, and comparison with those of $Sc_{5.5}Nb_{1.5}O_{12}$ ($a = 9.259(1)$ $c = 8.708(2)$ Å) suggests that these probably are the same phase.

The mixed-*Ln* compounds $YGdScSbO_7$, Nd_2ScNbO_7, and La_2ScNbO_7 were cubic phases with the pyrochlore structure, as confirmed by X-ray powder diffraction (Part II). The lattice parameters are given in Table III. (The use of electron diffraction patterns for identification of pyrochlore can be misleading, since similar patterns may arise from

domains of orthorhombic phase in several orientations within a single subcell orientation, or from crystals with the weberite structure.)

The pyrochlore structure, space group $Fd3m$, is adopted typically by $A_2B_2O_7$ compounds (*13*, *14*). There are two distinct cation sites, one occupied by A cations eightfold coordinated by O and the other by B cations in octahedral, i.e., sixfold, coordination. The B cations are necessarily smaller than the A cations. If the compounds Ln_2MO_7 have the pyrochlore structure, then the A and B sites must be occupied on average by different ratios of Ln and M ions. From the crystal chemistry of M ions, it is likely that they occupy only the B sites, so that a relevant pyrochlore will have the form $Ln_2(Ln'M)O_7$, with the Ln' and M ions randomly distributed on the B sites. It is clear that for the compounds studied here, only the Sc ion is small enough to occupy a B site as the cation Ln'.

Scandium showed little tendency to enter A sites in $Ln_2Ln'MO_7$ pyrochlores, even when accompanied by large Ln cations. Specimens of composition $LaSc_2NbO_7$(I) and $NdSc_2NbO_7$(II) were prepared by reacting together either the component oxides, or appropriate amounts of La_3NbO_7, Nd_3NbO_7, and "Sc_3NbO_7" at 1400°C for 7 days, followed by annealing at 1300 and 1200°C for 30 days. The method of preparation had no effect on the nature of the products. These were diphasic, I containing the phases $LaNbO_4$ and Sc_2O_3, and II consisting of a pyrochlore, a = 10.5019(4) Å (cf. Nd_2ScNbO_7; a = 10.5336(3) Å) and a phase similar to $Sc_{5.5}Nb_{1.5}O_{12}$, with parameters a = 9.269(1) and c = 8.710(1) Å.

Conclusion

The compounds Ln_3MO_7 examined in the present study have structures related to that of fluorite, the radius of the Ln cation having an important effect on the resultant structure type. When the Ln cation is large, an orthorhombic fluorite related superstructure is formed, of probable space group $Cmcm$ for Ln = La and $C222_1$ for Ln = Nd, Gd, Ho, or Y. For the smaller Er, and under some conditions, Ho and Y, the structure is that of fluorite with additional ordering effects possibly due to microdomains of an undetermined fluorite-related superstructure. Some evidence has been obtained that suggests that the orthorhombic materials transform to this fluorite type at high temperature.[1]

The pyrochlore structure reported earlier for compounds of this type was found only in the case of Ln_2ScMO_7, Sc being the only Ln ion small enough to occupy the site of octahedral symmetry necessary to this structure.

[1] A curious parallelism in structure types and unit cell dimensions appears for some rare earth rhenates, Ln_3ReO_8 (*15*). Here, an orthorhombic structure occurs for large Ln cations, with space group $Ccmm$ ($Cmcm$) for Ln = La, and $B22_12$ ($C222_1$) for Ln = Pr, . . ., Gd, and a cubic fluorite-type structure for Ln = Tb, . . ., Lu, and Y. Comparison of the detailed structures, when available, should be of interest.

References

1. H. P. Rooksby and E. A. D. White, *J. Amer. Ceram. Soc.* **47**, 94 (1964).
2. D. K. Nath, *Inorg. Chem.* **9**, 2714 (1970).
3. G. Boulon, J. P. Faurie, and C. Madej, *J. Solid State Chem.* **10**, 167 (1974).
4. J. P. Faurie, G. Boulon, and M. C. Delaigue, *J. Solid State Chem.* **17**, 7 (1976).
5. A. Byström, *Arkiv. Kem. Min. Geol.* **18A**, No. 21 (1945).
6. A. Byström, *Arkiv. Kem. Min. Geol.* **18B**, No. 10 (1945).
7. G. Tilloca, M. Perez y Jorba, and F. Queyroux, *C. R. Acad. Sci. Paris C* **271**, 134 (1970).
8. H. P. Rooksby and E. A. D. White, *Acta Crystallogr.* **16**, 888 (1963).
9. Z. A. Vladimirova, V. K. Trunov, and L. N. Komissarova, *Z. Neorg. Khim.* **15**, 2862 (1970) (*Russ. J. Inorg. Chem.* **15**, 1491 (1970)).
10. J. G. Allpress and H. J. Rossell, *J. Solid State Chem.* **15**, 68 (1975).

11. M. R. THORNBER, D. J. M. BEVAN, AND J. GRAHAM, *Acta Crystallogr. B* **24**, 1183 (1968).
12. H. J. ROSSELL, *J. Solid State Chem.* **19**, 103 (1976).
13. E. ALESHIN AND R. ROY, *J. Amer. Ceram. Soc.* **45**, 18 (1962).
14 F. BRISE AND O. KNOP, *Canad. J. Chem.* **46**, 859 (1968).
15. G. BAUD AND J. P. BESSE, *Mater. Res. Bull.* **9**, 1499 (1974).